FAKULTA
STROJNÍ
ČVUT V PRAZE

Department of Aerospace Engineering

Numerical simulation of selected trajectories in circumlunar and cislunar space

Numerická simulace vybraných trajektorií v cirkumlunárním a cislunárním prostoru

MASTER'S THESIS

2022

Ondřej HLADÍK

Studijní program: Letectví a kosmonautika
Studijní obor: 3906T008 Letadlová a kosmická technika
Vedoucí práce: Mgr. Jaroslav Kousal, Ph.D.

ZADÁNÍ DIPLOMOVÉ PRÁCE

I. OSOBNÍ A STUDIJNÍ ÚDAJE

Příjmení: **Hladík** Jméno: **Ondřej** Osobní číslo: **473542**

Fakulta/ústav: **Fakulta strojní**

Zadávající katedra/ústav: **Ústav letadlové techniky**

Studijní program: **Letectví a kosmonautika**

Studijní obor: **Letadlová a kosmická technika**

II. ÚDAJE K DIPLOMOVÉ PRÁCI

Název diplomové práce:

Numerická simulace vybraných trajektorií v cirkumulárním a cislunárním prostoru

Název diplomové práce anglicky:

Numerical simulation of selected trajectories in circumlunar and cislunar space

Pokyny pro vypracování:

1) Proveďte rešerši drah a manévrů pro přiblížení k Lagrangeovým bodům L4/L5 soustavy Země-Měsíc.
2) Vyberte možnosti přiblížení k 'ideálním' L4/L5 na vzdálenost pod 20000 km během období 1000 dní, se 'záchytem' a/nebo průletové. Zohledněte praktickou dostupnost počáteční trajektorie.
3) Realizujte vybrané trajektorie a manévry v numerické simulaci reálné (nekruhové) soustavy Země-Měsíc.
4) Charakterizujte realizované možnosti zejména s ohledem na potřebné delta-V, relativní rychlost vůči L4/L5 a dobu strávenou v jejich blízkosti.

Seznam doporučené literatury:

W. S. Koon, M. W. Lo, J. E. Marsden, S. D. Ross: Dynamical Systems, the Three-Body Problem and Space Mission Design, vydání 1.2, 2011
+ další literatura dle doporučení vedoucího

Jméno a pracoviště vedoucí(ho) diplomové práce:

Mgr. Jaroslav Kousal, Ph.D. ústav letadlové techniky FS

Jméno a pracoviště druhé(ho) vedoucí(ho) nebo konzultanta(ky) diplomové práce:

Datum zadání diplomové práce: **29.04.2022** Termín odevzdání diplomové práce: **08.06.2022**

Platnost zadání diplomové práce: _____

Mgr. Jaroslav Kousal, Ph.D.	Ing. Robert Theiner, Ph.D.	doc. Ing. Miroslav Španiel, CSc.
podpis vedoucí(ho) práce	podpis vedoucí(ho) ústavu/katedry	podpis děkana(ky)

III. PŘEVZETÍ ZADÁNÍ

Diplomant bere na vědomí, že je povinen vypracovat diplomovou práci samostatně, bez cizí pomoci, s výjimkou poskytnutých konzultací. Seznam použité literatury, jiných pramenů a jmen konzultantů je třeba uvést v diplomové práci.

.	
Datum převzetí zadání	Podpis studenta

Declaration

I declare that presented thesis called “Numerical simulation of selected trajectories in circumlunar and cislunar space” made under supervision of Mgr. Jaroslav Kousal, Ph.D., was written by me using literature listed in the chapter “Sources”

Acknowledgement

I am very thankful to my supervisor, Mgr. Jaroslav Kousal, Ph.D., for the opportunity to work on this project. I would also like to thank my friends, family, and especially to my girlfriend for always supporting me and helping me stay motivated.

Author:	Ondřej Hladík	
Title of thesis:	Numerical simulation of selected trajectories in circumlunar and cislunar space	
Title in Czech:	Numerická simulace vybraných trajektorií v cirkumlunárním a cislunárním prostoru	
Year:	2022	
Study program:	N3958 Letectví a kosmonautika	
Field of study:	3906T008 Letadlová a kosmická technika	
Department:	Department of Aerospace Engineering	
Thesis supervisor:	Mgr. Jaroslav Kousal, Ph.D.	
Bibliographic data:	Number of pages	31
	Number of figures	23
	Number of tables	1
	Number of attachments	0
Keywords:	Lagrange point, three-body problem, near-rectilinear halo orbit	
Klíčová slova:	Lagrangeovy body, problém tří těles, near-rectilinear halo orbit	

Abstract:

We have investigated potential transfer trajectories from NRHO to orbits in vicinity of triangular Lagrange points with aim being to find efficient trajectory, both in time of flight and Δv needed for maneuvers. We attempted to use already available solutions found within circular restricted three-body problem in our ephemeris simulation using GMAT. From our simulations we have found multiple potentially promising orbits around L5 with decreasing stability as shortest distance to Lagrange point decreases.

Anotace:

Prozkoumali jsme potenciální přechodové dráhy z NRHO na oběžné dráhy poblíž libračních bodů L4 a L5 s cílem minimalizace doby letu a nutného Δv. Pokusili jsme se použít již existující řešení pro kruhový omezený problém tří těles v efemerickém modelu simulace pomocí programu GMAT. Pomocí simulací bylo nalezeno několik slibných orbit v blízkosti bodu L5 se stabilitou snižující se s blízkostí průletů kolem Lagrangeova bodu.

Table of contents

1. Introduction

While most space missions are currently focused on low Earth orbit, it is not the only area of interest in relatively close proximity to Earth. Thanks to planned missions to vicinity of Moon, namely Lunar Gateway, that promise permanent presence and frequent transport. This opens new opportunities to study not only the Moon itself but also Lagrange points around it. It is necessary to harness this potential for scientific research while available as this lowers the cost of these missions and for lighter payloads offers convenient delivery as part of resupply mission. With this in mind comes the need to design missions with low total Δv and low total mass together with exploring options of transfer trajectories between different stable orbits in the region.

In this paper we have explored transfer trajectories for one such mission. The mission being worked on is tasked with investigation of Kordylewski dust clouds that are expected to be present around L4 and L5. We are launching from the NRHO orbit, same type of orbit as Lunar Gateway will inhabit, and aiming for horseshoe or tadpole orbit. We plan to conserve fuel by chaining several orbits together.

2. Motion of bodies

The movement of stellar bodies and man-made satellites is governed by Newton's Laws of motion and conservation of energy, as dissipating effects are vastly lower than in atmospheric flight. Thanks to low levels of energy dissipation we can consider total energy of a body, the sum of kinetic and potential energy, as invariant. Another simplification is offered for problems concerning man-made objects, as due to their negligible mass we do not have to consider their effect on other bodies, in these cases we refer to this problem as "restricted". [1] [2]

2.1. The two-body problem

The simplest of problems we can encounter in astrodynamics considers relative motion of two bodies. It is also the most complex problem that offers an analytical solution. Equations of motions have the form of

$$\ddot{\boldsymbol{r}}_{\mathbf{1}} = G\frac{m_2\boldsymbol{r}}{r^3} \tag{1}$$

$$\ddot{\boldsymbol{r}}_{\mathbf{2}} = -G\frac{m_1\boldsymbol{r}}{r^3} \tag{2}$$

Where $\boldsymbol{r}$ is positional vector of body corresponding with its subscript and relative positional vector, and m is mass of the body. In few steps we can get the equation of relative motion as [1]

$$\ddot{\boldsymbol{r}} = -\mu\frac{\boldsymbol{r}}{r^3} \tag{3}$$

$$\mu = G(m_1 + m_2) \tag{4}$$

In many cases, especially when concerning man-made objects, one of the masses is several orders of magnitude lower than the other. As even the ISS, weighing over 419 tons [3], has negligible mass compared to Earth and Moon, we can safely assume our probe's mass and its gravitational pull can be disregarded.

Two body-problem is insufficient for our purposes as our probe orbits the moon and Lagrange points of Earth-Moon system. Therefore, this short explanation of two-body problem serves only as stepping-stone to our main theoretical topic.

2.2. The three-body problem

Three-body problem in its entirety is several steps more complicated than two-body problem, which is the reason we introduce many simplifications, the most important for us remaining restricted three-body problem due to low relative mass of our probe.

The simplest variant of three-body problem is circular planar restricted three-body problem. Despite the level of simplification from real case, it still offers very valuable information. Since the bodies are restricted to movement on plane, we operate on a plane, commonly in inertial rotating frame, as shown in Figure 1. [1]

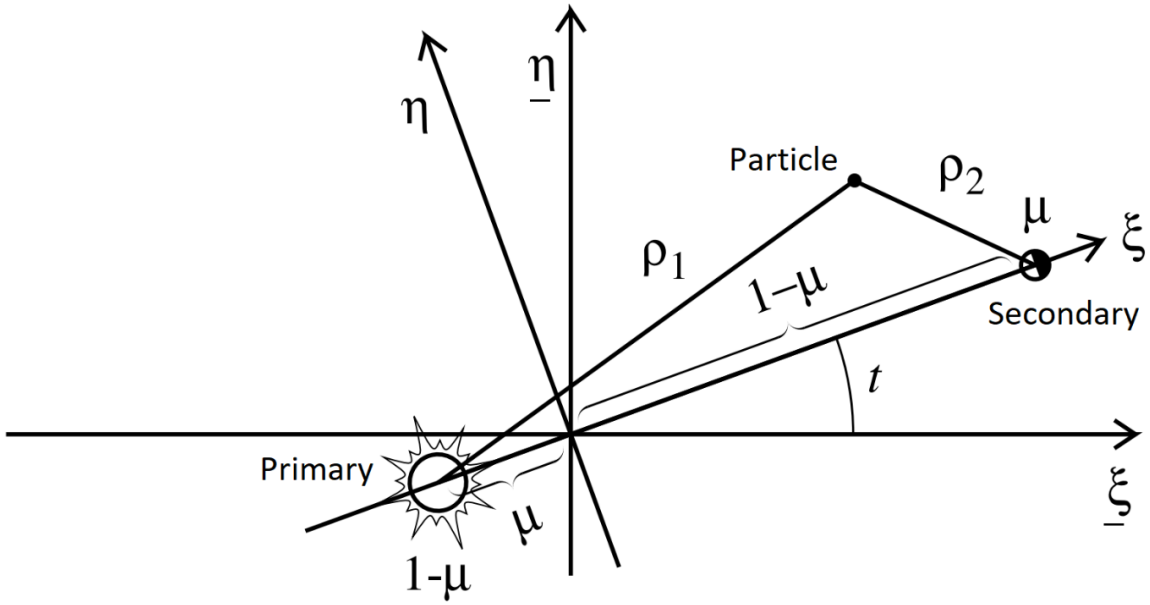

Figure 1 - Inertial rotating frame of restricted three-body problem [1]

The center of the inertial frame is usually in the barycenter of the system, which can often be very close to the center of mass of primary body. To decrease number of variables we use so called "unit of mass" which is sum of the masses of primary and secondary body, then we can write mass of secondary body as μ and mass of primary as $1-\mu$. The distance of those bodies to the barycenter hosting the center of inertial frame is then inverse of the masses, μ for primary and $1-\mu$ for secondary with unit of length being distance between primary and secondary body. Inertial rotating frame has one major advantage in keeping position of primary and secondary body as constant in circular three-body problem, or their motion usually linear if secondary body is on elliptical trajectory. [1]

Hamiltonian equation [1] in this inertial frame is

$$H = \frac{1}{2}\left(P_\xi^2 + P_\eta^2\right) + P_\xi\eta + P_\eta\xi - \frac{1-\mu}{\rho_1} - \frac{\mu}{\rho_2} \tag{5}$$

From which we can, after several steps, get equations of motion [1] as

$$\ddot{\xi} - 2\dot{\eta} = \frac{\partial\Omega}{\partial\xi} \tag{6}$$

$$\ddot{\eta} + 2\dot{\xi} = \frac{\partial\Omega}{\partial\eta} \tag{7}$$

With Ω being an effective potential of our particle. [1]

$$\Omega = \frac{1}{2}(\xi^2 + \eta^2) + \frac{1-\mu}{\rho_1} + \frac{\mu}{\rho_2} \tag{8}$$

From the equations of motion, we can compute some of the crucial constants of our system, by expanding motion equations with $\dot{\xi}$ and $\dot{\eta}$ respectively [1]

$$\ddot{\xi}\dot{\xi} - 2\dot{\eta}\dot{\xi} = \frac{\partial \Omega}{\partial \xi}\dot{\xi} \tag{9}$$

$$\ddot{\eta}\dot{\eta} + 2\dot{\xi}\dot{\eta} = \frac{\partial \Omega}{\partial \eta}\dot{\eta} \tag{10}$$

Then we add these equations together [1]

$$\ddot{\xi}\dot{\xi} + \ddot{\eta}\dot{\eta} = \frac{\partial \Omega}{\partial \xi}\dot{\xi} + \frac{\partial \Omega}{\partial \eta}\dot{\eta} \tag{11}$$

$$\frac{d\dot{\xi}}{dt}\dot{\xi} + \frac{d\dot{\eta}}{dt}\dot{\eta} = \frac{\partial \Omega}{\partial \xi}\frac{d\xi}{dt} + \frac{\partial \Omega}{\partial \eta}\frac{d\eta}{dt} \tag{12}$$

$$\frac{d}{dt}\left(\dot{\xi}^2 + \dot{\eta}^2\right) = 2\frac{d\Omega}{dt} \tag{13}$$

By integrating this equation, we get [1] [2]

$$\dot{\xi}^2 + \dot{\eta}^2 = v^2 = 2\Omega - C \tag{14}$$

Where C is a constant called the Jacobi integral [1] and since v^2 can't be negative, we can write inequation

$$2\Omega - C \geq 0 \tag{15}$$

Or

$$\Omega \geq \frac{C}{2} \tag{16}$$

And since the Jacobi integral is constant, we can evaluate it if we know position and velocity for any moment of flight of the particle. Further, Ω is only a function of its position, so we can compute what position the particle can assume without violating the inequation. [1] [2]

2.2.1. Lagrange points

With inequation mentioned previously, we can chart areas that the particle can't occupy with given value of Jacoby integral [1]

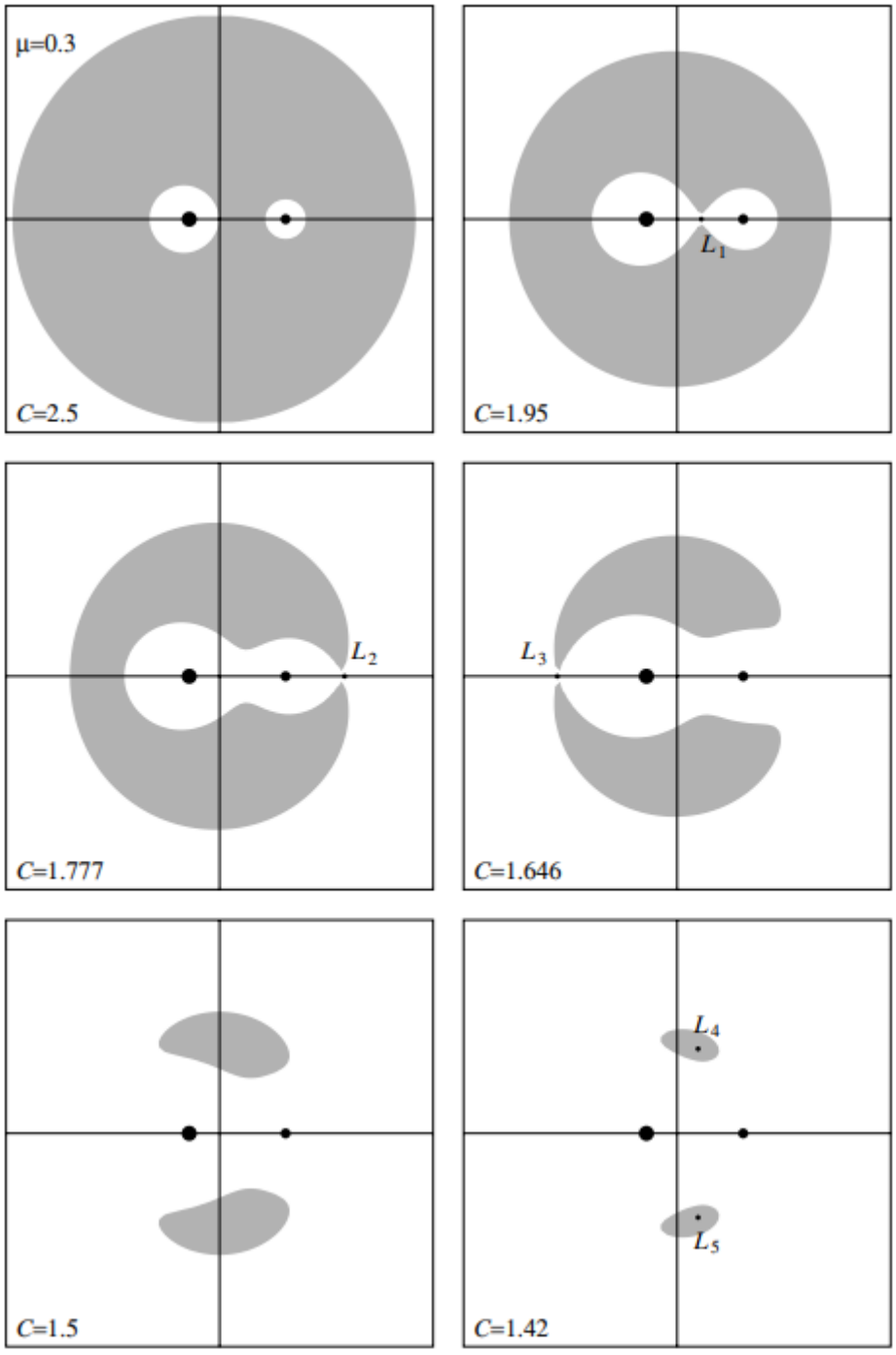

Figure 2 - Forbidden zone (grey) depending on value of the Jacobi integral for $\mu = 0.3$ [1]

We can see in Figure 2 that for high values of C the particle can enter area close to the primary and secondary body or circular area far away from both. Depending on μ and C, these areas can also show us where two-body problem is sufficiently accurate, either due to being close enough to one of the bodies to be able disregard effects of the other, or

far enough to view the two bodies as one entity. We also can safely say that the orbit of the body is stable if it is within one of the two inner areas as it can never escape from the system. With dropping value of the Jacobi integral we see the two roughly circular areas deform and connect, with first point of contact between two inner accessible areas being labeled L1. This new internal area means that primary and secondary can trade satellites. [1] [2]

As we further decrease C we see the outer area connect with inner on in point labeled L2. Leaving the forbidden zone in roughly horseshoe shape until it becomes cut into two pieces as internal allowed area expands to contact the external one at point L3. Then with further decrease in the Jacobi constant the two remaining areas shrink into tadpole or kidney shaped areas until only points L4 and L5 remain. [1] [2]

So what are those points and why are they of such interest to us? By looking at the gray forbidden zone we can see that these points are most definitely local extremes of effective potential function Ω of which we know the previously mentioned inequality (16). This paired with the fact that Ω achieves maximal values in infinite distance from both objects and at the point masses used to represent our primary and secondary, means that the points we are seeing are saddle points, in case of L1, L2, and L3, and global minima for L4 and L5. This means all of these points allow for equilibrium to be reached and particle suspended at them to remain stationary in relation to primary and secondary body within inertial rotating frame, there is still question of stability of this equilibrium. [1] [2]

For L1, L2, and L3, the saddle points, it has been mathematically proven that they are unstable equilibrium points [1], as could be expected from saddle points. It is more interesting for global minima in points L4 and L5, as the stability of those depends on value of μ [1], for those points to be stable inequality that needs to be satisfied is

$$\mu < \frac{1}{2} - \sqrt{\frac{23}{108}} \approx 0.0385 \tag{17}$$

As the Earth-Moon system is of interest to us we can quickly check if L4 and L5 of this system are stable within our simplified example, where μ represents relative mass of Moon to the whole system, therefore

$$\mu = \frac{m_M}{m_E + m_M} = \frac{7.348 \cdot 10^{22}}{5.972 \cdot 10^{24} + 7.348 \cdot 10^{22}} \approx 0.0122 \tag{18}$$

From this we see that our L4 and L5 should be stable, which is supported by observation of Kordylewski dust clouds. These dust clouds have been observed at both L4 and L5 with more observations happening around L5. [4]

2.3. Types and families of orbits

As orbits that are solution to three-body problem are often very different to simple circular or elliptical trajectory, they have been categorized into groups based on various parameters, usually related to nearby Lagrange points and bodies. While there is very large number of such categories, we will focus on the ones that are or have been of interest to us. [5] [6]

2.3.1. Distant retrograde orbit

These orbits are coplanar to the Moon's orbit around Earth. These orbits are exceptionally stable and can reach far beyond L1 and L2, even going close to Earth. This offers great diversity of coordinates that can be reached on these orbits. [5]

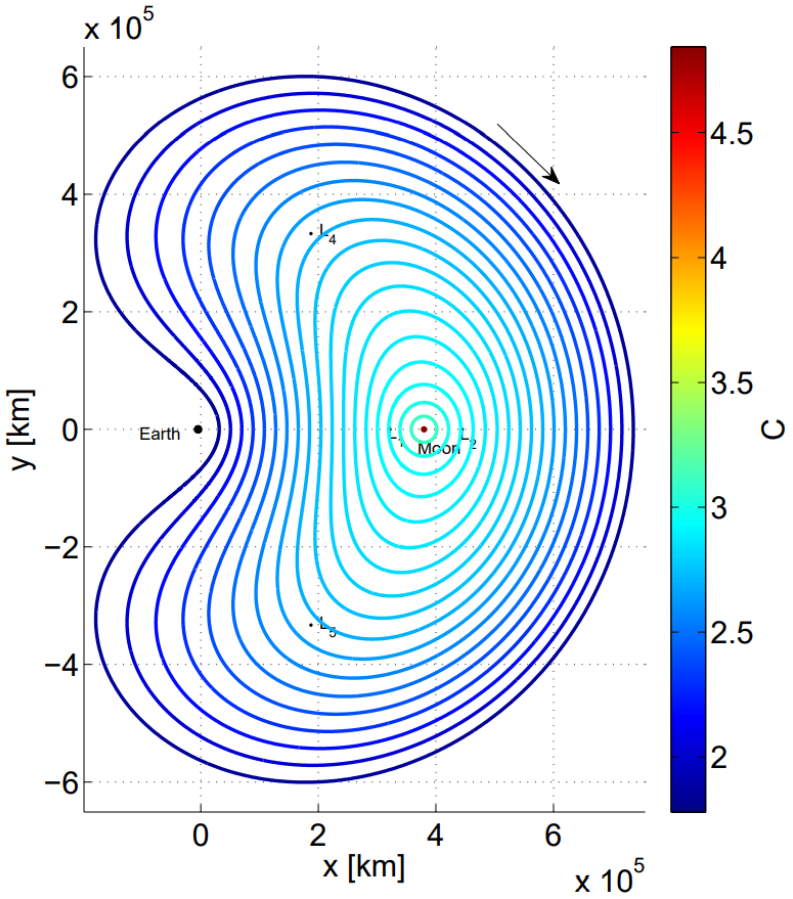

Figure 3 - Distant retrograde orbits of Moon, color denoting value of the Jacobi constant [5]

As we can see in Figure 3, the area which is covered by trajectories of distant retrograde orbits is considerable. Their main disadvantage is that being coplanar with Moon's orbit around Earth satellites can find themselves not only entering shadow of the Moon, it can also find itself in Earth's shadow and as these orbits have long periods it might lead to extended time spent without power being generated via solar panels. As this disadvantage can be solved with proper planning, the exceptional stability and transfer options outweigh it.

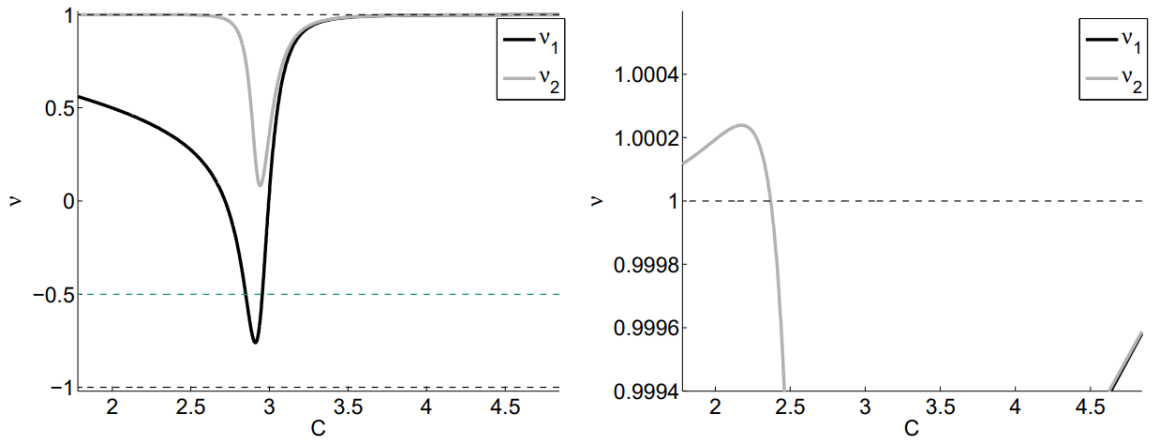

Figure 4 - Stability indices for distant retrograde orbits depending on value of the Jacobi constant [5]

As can be seen in Figure 4, the trajectory is stable for $C > \sim 2.369$, with planar stability (υ_1) being especially good, and slightly more sensitivity to out of plane disturbances. [5]

On example of distant retrograde orbit, we will also explain how families of orbits are found and described, as it can be easily explained on it. We start with initial conditions of $[x_0, 0, 0, 0,\ \dot{y}_0, 0]^T$ where $\dot{y}_0$ is varied until our particle perpendicularly crosses x-axis on the other side of the Moon. Then for the next orbit in the family we use the solution of $\dot{y}_0$ as initial guess and small variation to x_0. Similar methods are used for all other families of orbits with variation of what parameters are being used and what are criteria for such orbits. [5]

2.3.2. Near rectilinear halo orbit

Halo orbits were first described in 70s as an option for translunar coverage without being obstructed by the Moon. Nowadays we can speak of three main types of halo orbits that are in separated by being in vicinity of different Lagrange points, L1, L2, and L3. Of interest to us are only the L1 and L2 families. These are present near the Moon and are interesting due to offering relatively easy transfer from Earth and transfer to other orbits. From halo orbits a specific family can separated, near-rectilinear halo orbits. These orbits come close to Moon on either the north or the south pole, above which their periapsis is located. [5]

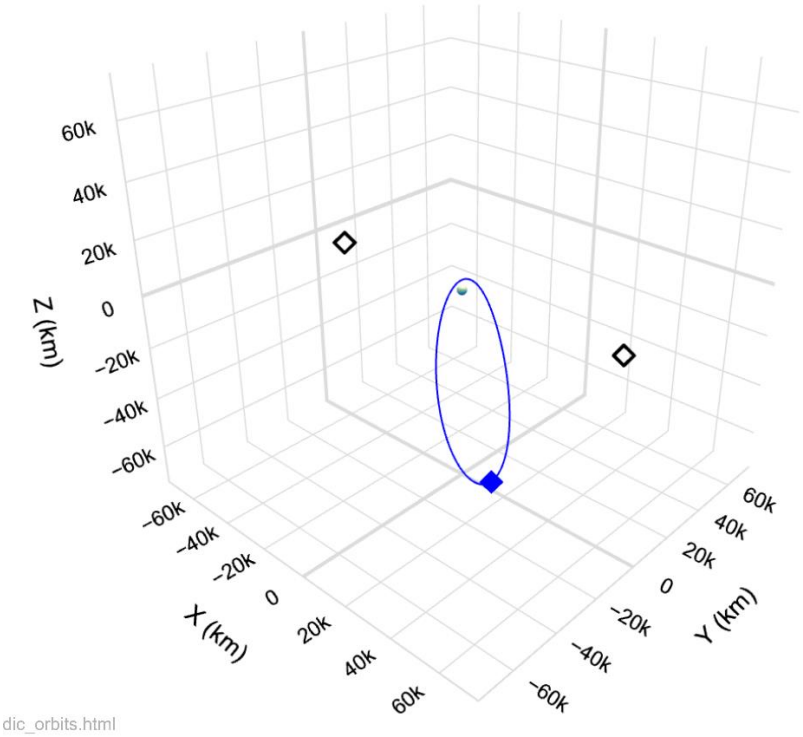

Figure 5 - Southern L2 near-rectilinear halo orbit used for simulations in this paper, Earth in direction of negative X axis [7]

Further, we can see in Figure 5 that the trajectory slightly curves towards the L2 point, but remains almost perpendicular to Moon's orbital plane, which makes its trajectory resemble an ellipse. That is a characteristic separating NRHOs from other halo orbits. [6]

The stability of these orbits has been studied within circular restricted three-body problem, where it has been found that some of L2 halo orbits can be stable as seen in Figure 6. [5]

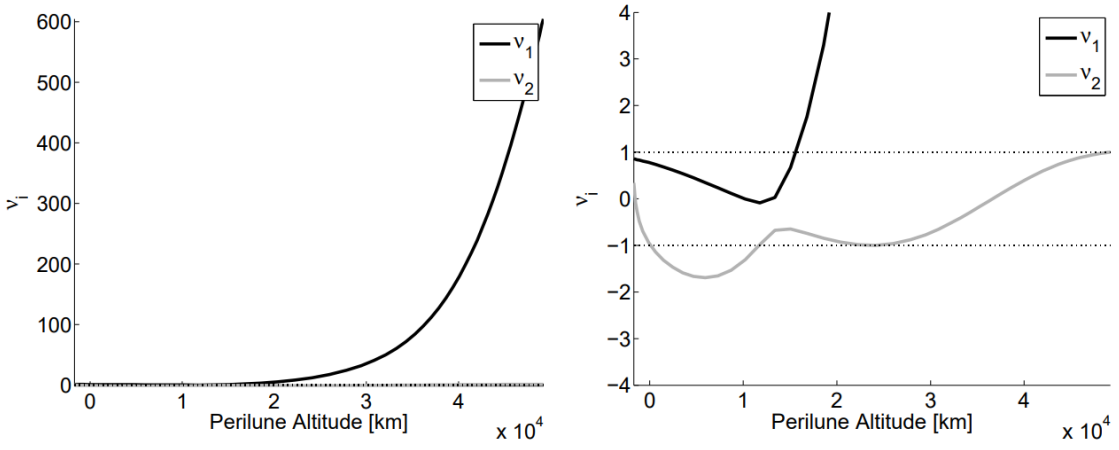

Figure 6 - Stability indices for L2 halo orbits, for stability both indices need to have absolute value of less than 1 [5]

Since L2 near rectilinear halo orbits are characterized by periapsis, in our case perilune, ranging from 1850 km to 17350 km and periods from roughly 6 to 10 days, we can see that within this simplified three-body problem they can be stable. The upside to NRHO

even outside of marginally stable ones is that divergence rate is significantly slower than when compared to other orbits. [6]

As has later shown in simulations, since most of the sources use circular restricted three-body problem, the accuracy of prediction of stability of our particular orbit seems to differ from results of the simulation. This can be attributed to both movement of Moon as well as Lagrange points. It is possible that this could be partially rectified by some appropriate changes to velocity vector of our probe. [5] [6]

For us Southern L2 near-rectilinear halo orbit presents ideal position to start our mission, as thanks to such orbit soon housing space station Lunar Gateway, we can expect many flights towards its orbit. Furthermore, halo orbits in general offer a good opportunity for transfer to many of the nearby orbits.

2.3.3. Orbits around L4 and L5

These orbits are related to triangular Lagrange points, L4 and L5. Tadpole orbits, named for their shape, stay in neighborhood of one Lagrange point, while horseshoe orbits travel between L4 and L5 over L3. [8]

First, we will look at families of planar horseshoe orbits. These orbits exist with the Jacobi constant allowing escape of particle to outer plane. In Figures 7, 8, and 9 we can see examples of three families of horseshoe orbits. For clarity only half of the symmetrical orbit is shown. [8]

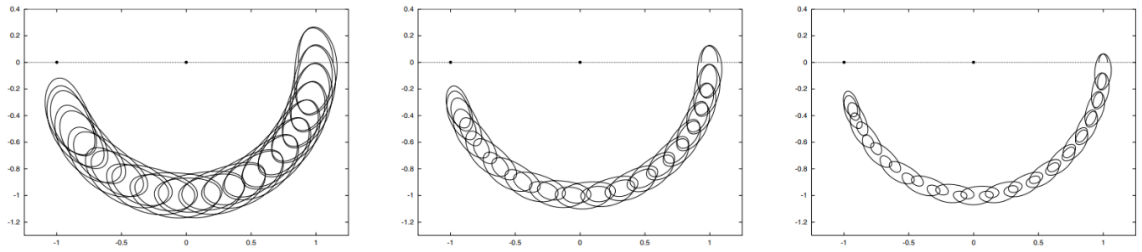

Figure 7 - Examples of "A" family of horseshoe orbits [8]

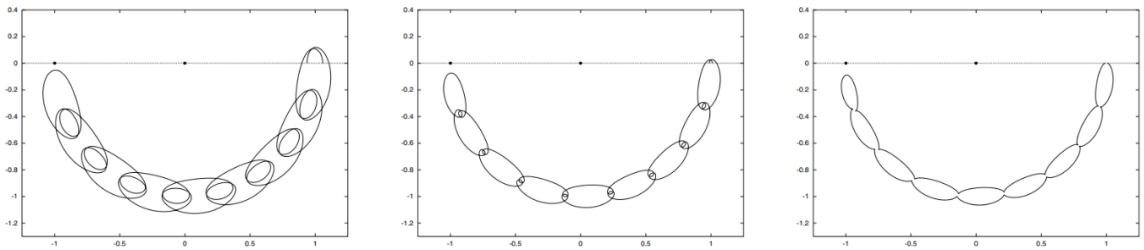

Figure 8 - Examples of "B" family of horseshoe orbits [8]

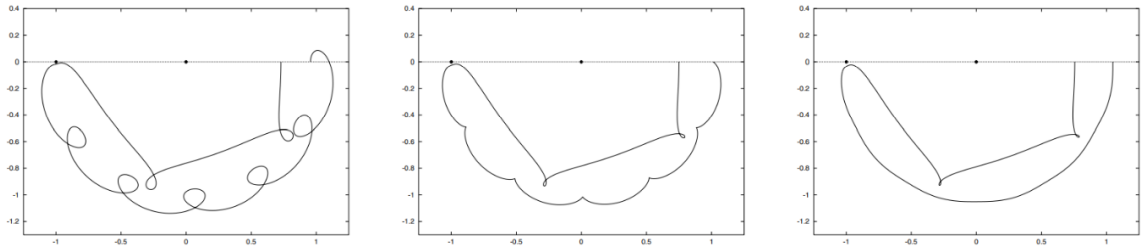

Figure 9 - Examples of "C" family of horseshoe orbits [8]

As we can see, objects on these orbits will spend most of the time far away from L4 and L5, which makes these orbits less desirable for us. The upside is stability of those orbits which, in scope of circular restricted three-body problem, is good. But even improved orbital stability doesn't make up for far too long periods, sometimes even several decades, especially in "A" family. [8]

For us far more interesting are orbits that stay close to one of the Lagrange points without excessive time spend in flight between L4 and L5. This means we will be considering orbits closer to those of Trojans and Greeks. Orbits around L4 and L5 can be split between Short period orbits and Long period orbits as depicted in Figure 10. [5]

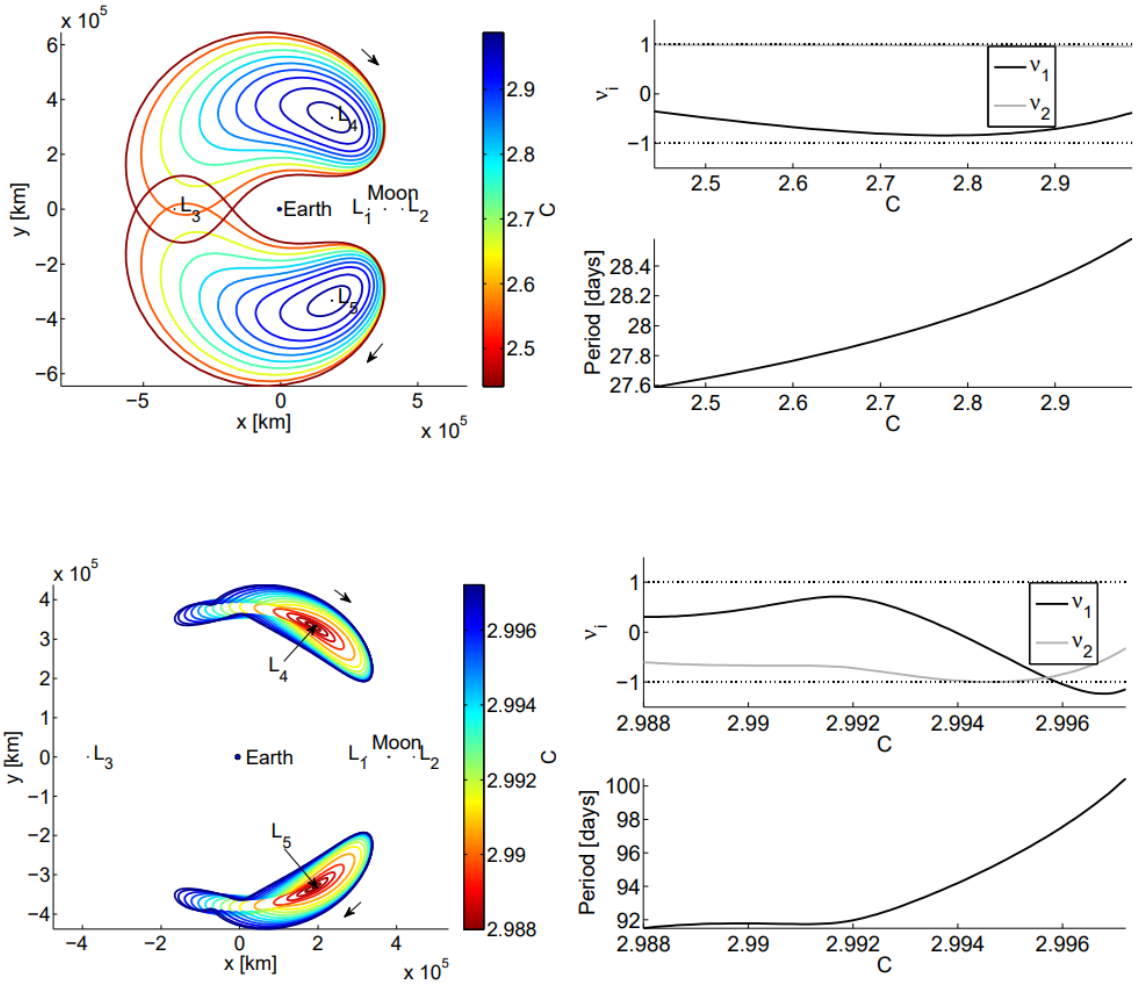

Figure 10 - Shape, energy, and stability of various short (upper) and long (lower) period orbits [5]

As can be seen, short period orbits increase in energy as they get further away from Lagrange points, while long period orbits increase in energy with proximity to them. In addition, all of the shown short period orbits are stable, as stability indices stay within acceptable absolute value (dotted line in the graph), while long period orbits appear to lose stability when they get too far from the Lagrange point. [5]

Stability of Short Period Orbit together with its short period that ensures that even if part of orbit is too far from the Lagrange point we will still be able to achieve reasonable portion of time spent close to our target location.

2.4. Orbit chaining

When choosing a transfer trajectory to our target orbit we should also investigate options of chaining several changes of orbit together. This allows us to utilize our probe's energy better. We can both save fuel and time by choosing correct intermediate trajectory. To help us determine beneficial choices for chaining orbits we can use the Jacobi constant since it is an energy-like constant. We know that the probe must pass through all the values of C between the initial C_0 and the final C_f. The Jacobi constant is function of position and velocity with it being constant on every orbit. This means we can utilize orbits with clues of the Jacobi constant in-between our initial and final value. Therefore, the first step to creating a working orbit chain is investigating the Jacobi constants of our orbits and searching out orbits with the Jacobi constant between our launch and target orbits. [9]

Once we assemble our chain of orbits we can then focus on choosing optimal transfers both from perspective of time and energy cost. This is very complicated, as determining the optimal transfer is not possible with every set of initial values, which leads to creation of families of transfer trajectories. Further, some transfers are available only under certain relative positions of probe to primary and secondary. While there is no upper limit to number of intermediate orbits, and often there can be a large number of them, we will take look at short three-link orbit chains as examples in Table 1. [9]

Table 1 - Time of flight, change in velocity and mass, and mass fraction for spacecraft with initial mass of 1 ton and specific impulse of 2000 seconds [9]

Transfer Type	$TOF\ (days)$	$\Delta m\ (kg)$	m_f/m_0	$\Delta v\ (m/s)$
DRO → L_4 SPO → L_3 Lyapunov	70.0966	32.6313	0.9674	650.6823
DRO → 2:3 Resonant → L_3 Lyapunov	91.5769	30.2737	0.9697	602.9403
L_2 Lyapunov → P3DRO → DRO	94.1852	7.9340	0.9921	156.2332
L_2 Lyapunov → DPO → DRO	74.7037	5.5744	0.9944	109.6388
NRHO → 2:3 Resonant → DRO	121.3350	12.9961	0.9870	256.5670
NRHO → Butterfly → DRO	57.6456	24.1019	0.9759	478.5069

We can see that correct choice of intermediate orbit is crucial for optimal transfer and that decrease in time of flight doesn't always correspond with increase in Δv. And the complexity rises with each added link to our orbit chain, so while there is no theoretical upper limit to amount of orbits that can be chained together, we will quickly run into one

caused by time and computing capacity. Further, we are also heavily limited by our own knowledge of orbits and good initial values for transfers between them. This means that experience and intuition are still very much a crucial part of trajectory design despite many attempts at finding ways to bridge this gap. [9]

2.5. Transfer Network

As was said in the previous chapter there is never one single solution to transfer between two orbits, even without chaining orbits together. This is due to the same reasons why we have many orbits that can differ wildly. Therefore, transfers are grouped into families just like orbits are. This is the reason why correct initial guess is critical when not using well mapped transfer network, as we can find ourselves with suboptimal solutions, especially in cases when there is lack of experience with such transfer trajectory designs. [5]

Transfer networks are usually created between set orbits, therefore the first step in creation of such transfer network is choosing which orbits we want to connect, because while it is safe to assume that similar enough orbits will have relatively similar transfer trajectories, transfer networks attempt to provide an exact solution, and even when we remain in same family of orbits, the optimal transfer trajectory might shift outside of the vicinity of the initial guess provided as solution in transfer network. [5]

Transfer networks are a powerful tool for simplifying both transfer between orbits and their chaining and making transfer design more accessible by partially removing the hurdle in the form of the initial guess of position and velocity [9]. In theory if we have an expansive and complex enough transfer network, we might be able to create ideal transfers between two orbits in three-body problem. Regrettably, such a complex transfer network is, at least at the moment, not available.

3. Development of transfer trajectory

We have set NRHO as our starting orbit with aim of achieving SPO around one of the triangular Lagrange points. Our aim was to achieve the lowest possible Δv while maintaining transfer time below a thousand days. Our aim was to achieve $\Delta v < 500\ \mathrm{m\ s^{-1}}$. Our target orbit has to pass closer than twenty thousand kilometers away from either of the triangular Lagrange points, L4 and L5, ideally be captured within such distance for the entire time.

3.1. First transfer chain proposition

Initially we have been searching for already tried and tested solutions, or already fully explored ones. We found a promising transfer network [5] utilizing DRO as central hub for transfers to and from all other orbits. For us, the transfers from NRHO and to SPO at vicinity of L4 and L5 were crucial.

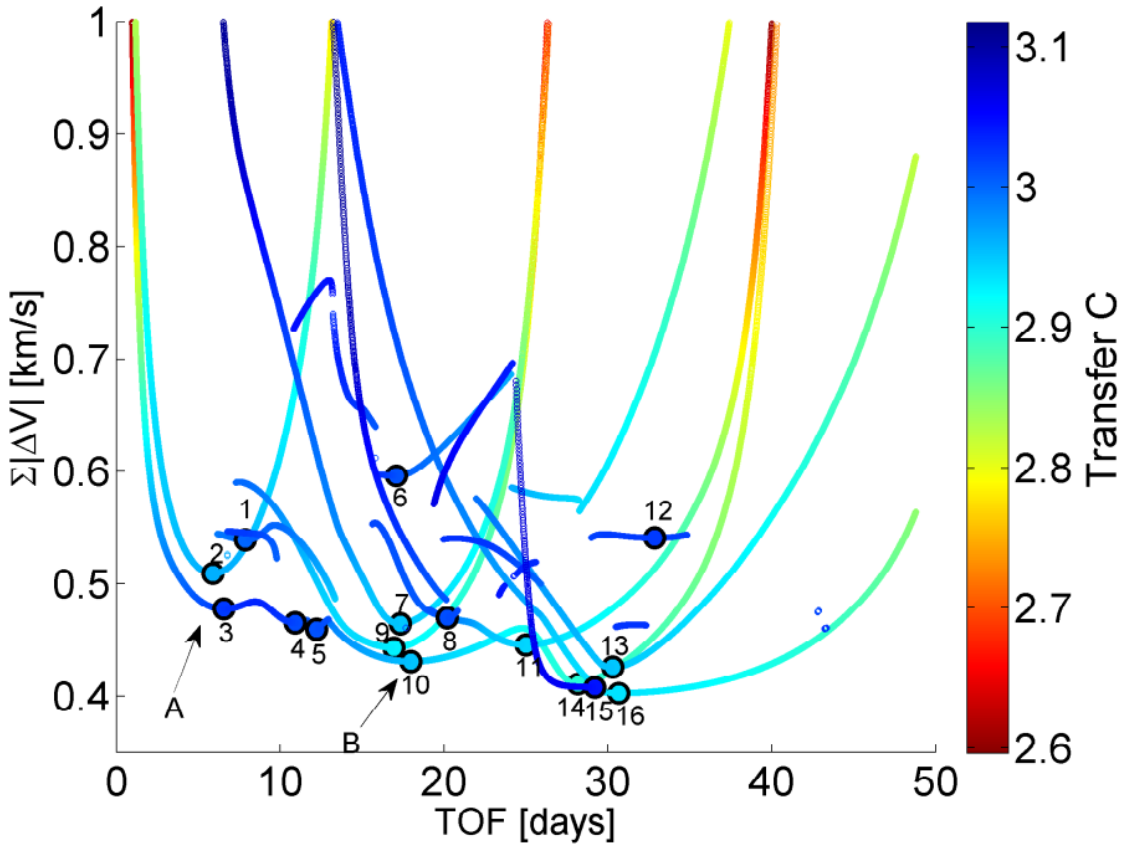

Figure 11 - Transfer options from L2 NRHO to DRO [5]

First, we investigated our options for transfer to DRO from NRHO. As can be seen in Figure 11, we have multiple options and all of the transfers are well within acceptable time of flight. This means we choose the transfer trajectory labeled as 16. This transfer takes slightly over 30 days [5] to reach its target trajectory at cost $\Delta v = 402.62\ \mathrm{m\ s^{-1}}$[5]. When looking at the trajectories as shown in the next figures, chosen as extreme examples of transfer trajectory, comparing the most energy efficient trajectory 16, Figure 12, that we

chose with the least effective trajectory 6, Figure 13. We can clearly see reason for the better energy efficiency of our chosen transfer. The direction of velocity the probe possesses aligns much better in our chosen transfer than in transfer 6, where only a fraction of the velocity compounds beneficially with the target velocity after the maneuver. This is not surprising, as this can be observed even in simple Hohmann transfer and is principally why change in orbital inclination can be considered the worst maneuver energetically. From this, we determined that if we have to develop our own transfer trajectories, we should always attempt to use velocity changes that are as close as possible to the direction of our current velocity vector. [5]

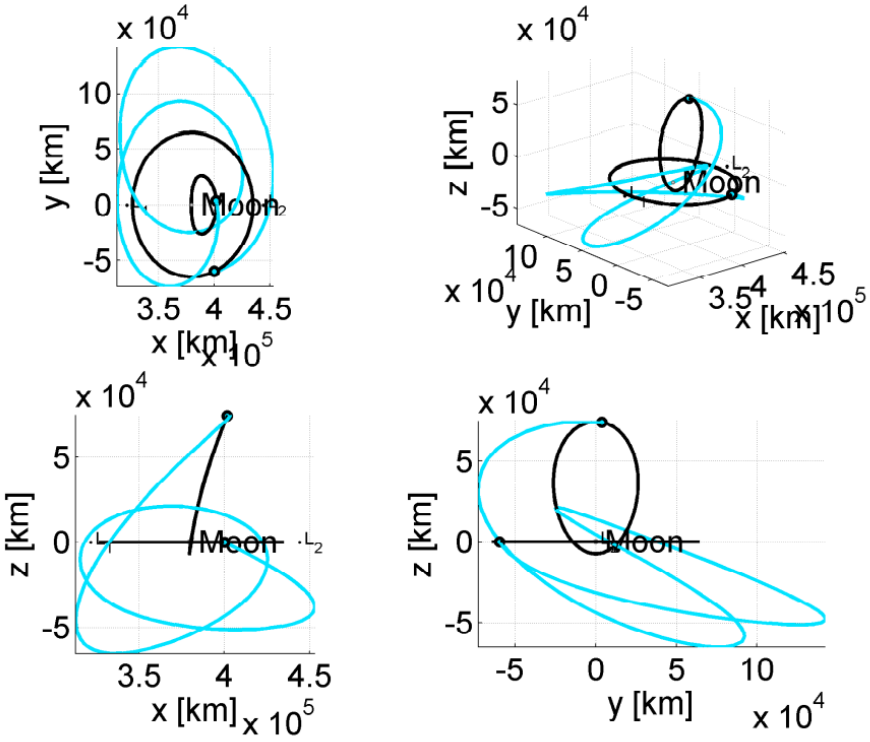

Figure 12 - Flight path of transfer 16 [5]

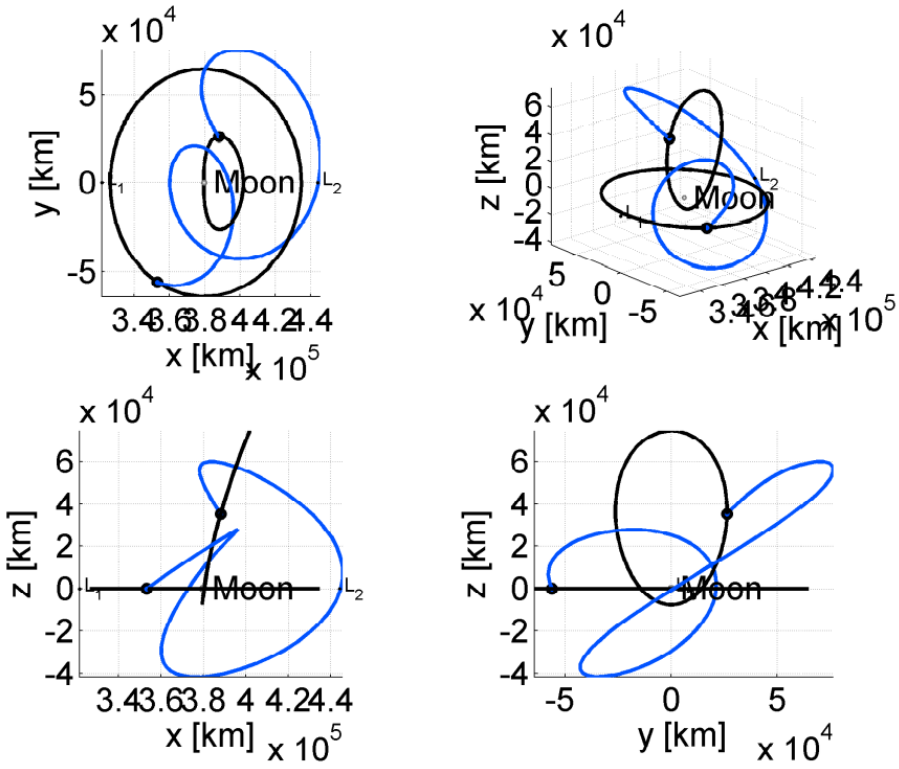

Figure 13 - Flight path of transfer 6 [5]

The second transfer would be from DRO to SPO. We had the option of choosing between L4 and L5. As there is no major difference for us in either of those locations, we opted to decide depending on the transfer availability and the Δv needed.

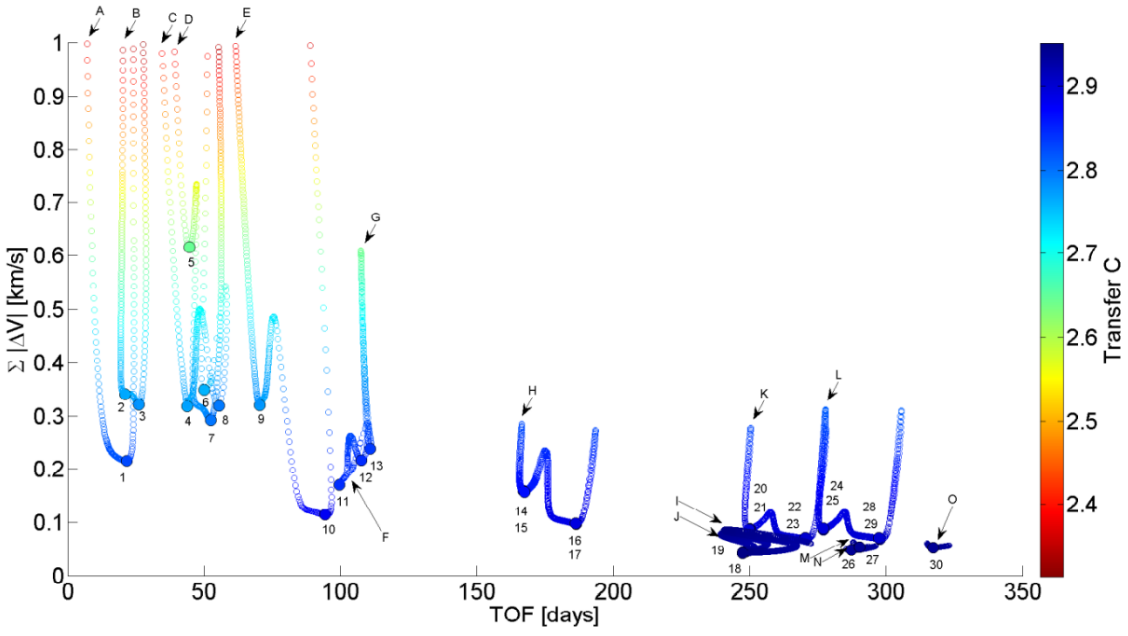

Figure 14 - Graph of needed change in velocity based on time of flight of transfer trajectories between DRO and L4 SPO [5]

First, we look at transfers between DRO and L4 SPO which have their time of flight and Δv shown in Figure 14. We can see that flight time is much more considerable for these transfers, but the needed change in velocity is much lower than for transfer from NRHO to DRO. We have chosen transfer I18, which takes approximately 247 days with $\Delta v = 42\ \mathrm{m\ s^{-1}}$. [5]

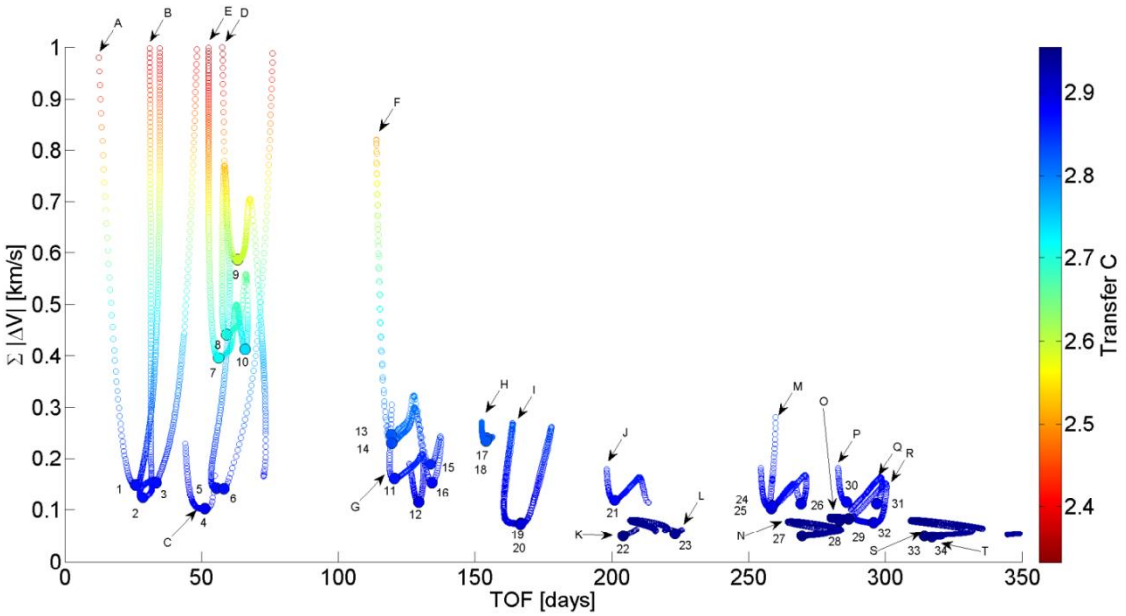

Figure 15 - Graph of needed change in velocity based on time of flight of transfer trajectories between DRO and L5 SPO [5]

When we look at transfers between DRO and L5 SPO, we notice that optimal transfers to L5 SPO take longer than to L4 SPO. From the transfer options shown in Figure 15, T34 appears to be the best when it comes to needed velocity adjustment at $\Delta v = 47.5\ \mathrm{m\ s^{-1}}$ and requiring 317 days. [5]

While these transfers are close in their monitored parameters, transferring to L4 SPO appeared to be better choice due to both being lower in Δv and requiring less time.

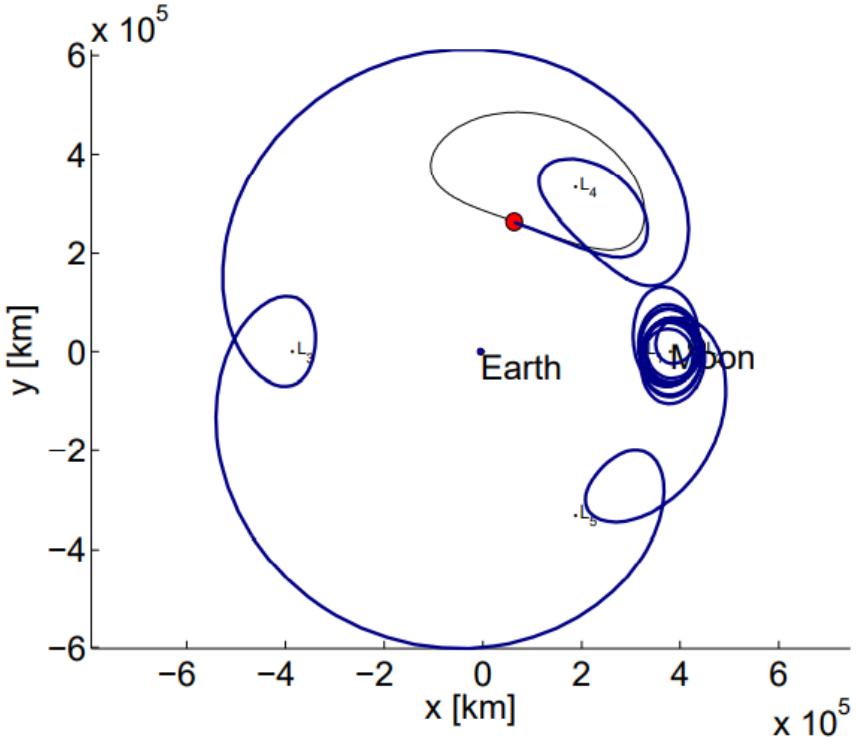

Figure 16 - Trajectory of chosen transfer between DRO and L4 SPO [5]

As this transfer is planar, we can see it in its entirety in Figure 16. After the initial maneuver, the probe slowly drifts out of DRO followed by fly-by of L5 and L3 before the trajectory aligns very closely with L4 SPO and allows achieving that orbit with minimal expense of fuel. [5]

In total, these transfers chaining NRHO-DRO-L4 SPO, would cost $\Delta v = 444.62\ \mathrm{m\ s^{-1}}$, which would satisfy our initial aim of less than $\Delta v < 500\ \mathrm{m\ s^{-1}}$ and transfer time should also be satisfactory, since periods of NRHO and DRO are not long enough to greatly affect length of the transfer and transfers themselves add up to 345 days.

This initial proposition has several problems. First the target orbit is not optimal for us and we would need to adjust it closer to L4, but this pales in comparison to the fact that this transfer network has been designed in circular restricted three-body problem, which means that accuracy of these predictions for non-circular three-body problem is not guaranteed.

While this plan was ultimately found less viable it has been an important stepping-stone in development of our final trajectory.

3.2. General mission analysis tool

Before talking about the simulations themselves, we need to talk about the software used for them. We were using General Mission Analysis Tool (GMAT) developed by NASA. It is being used widely within industry by government agencies, universities, and private

companies. GMAT is available as open-source software making it ideal for academic applications. [10]

As the name suggests, GMAT is software for mission analysis. This means that we can use it to inspect the trajectory of our probe and plan our maneuvers. The level of detail of the simulation can be adjusted, with option of selecting which bodies' gravitational effect is to be taken into account as well as solar radiation pressure. This allows optimizing which parameters have big enough effects on our mission. GMAT also offers a range of solvers to help with creating transfer trajectories and other optimization tasks. Trajectories of celestial bodies are modeled using ephemerides, giving GMAT the greater accuracy it needs over circular three-body problem solution that might be used otherwise. [10]

In our simulations we are using a rotating frame with its center corresponding to the Earth's center of mass.

3.3. Launch orbit

When our first attempts at creating the models within GMAT were made we quickly discovered that solutions available for stable near-rectilinear halo orbits that are available as solution for circular three-body problem are not viable in ephemeris model used by GMAT as can be seen in Figure 17.

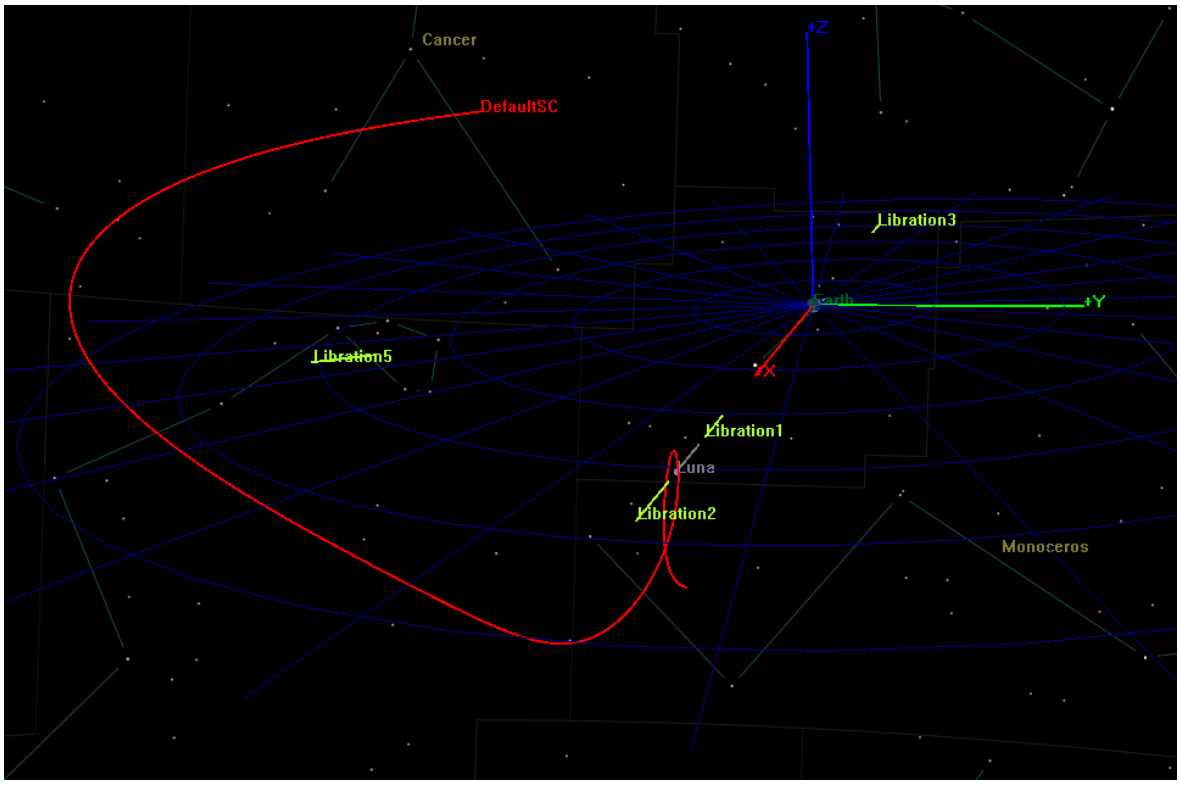

Figure 17 - Flight path of probe without correcting its orbit for Moon's eliptical orbit

We believe the reason was that the Moon was not static and was moving along the x-axis to and from Earth which introduced disturbances to our NRHO orbit. We have tested several of the solutions stable in circular restricted three-body problem, and none of the attempts were successful. Which led to needing to stabilize the orbit first. We have

attempted to stabilize several of the orbits. We were the most successful in the case of orbit seen in Figure 5. This orbit has its aposelene at 72 820 kilometers away from the Moon and comes as close as 3 625 kilometers in its periselene, with period of 6.8 days.

To stabilize the orbit, we decided to use impulse maneuver, which we prescribe Δv for braking maneuver, negative y-axis. This has proven to be a fast and successful approach. Because due to nature of "Target" function we were unsuccessful in creating parameters within which solver would successfully converge giving us stable, or temporarily stable orbit, we had to use manual iterations, which have ultimately landed us on $\Delta v = 74.15\ \mathrm{m\ s^{-1}}$. With that we have managed to successfully stabilize the orbit for roughly 35 days before it diverges too far and we lose orbit around the Moon. This can be seen in Figure 18, showing that the probe first completed about 5 revolutions around the Moon before it lost orbit as the Moon started to move towards Earth after passing its apogee.

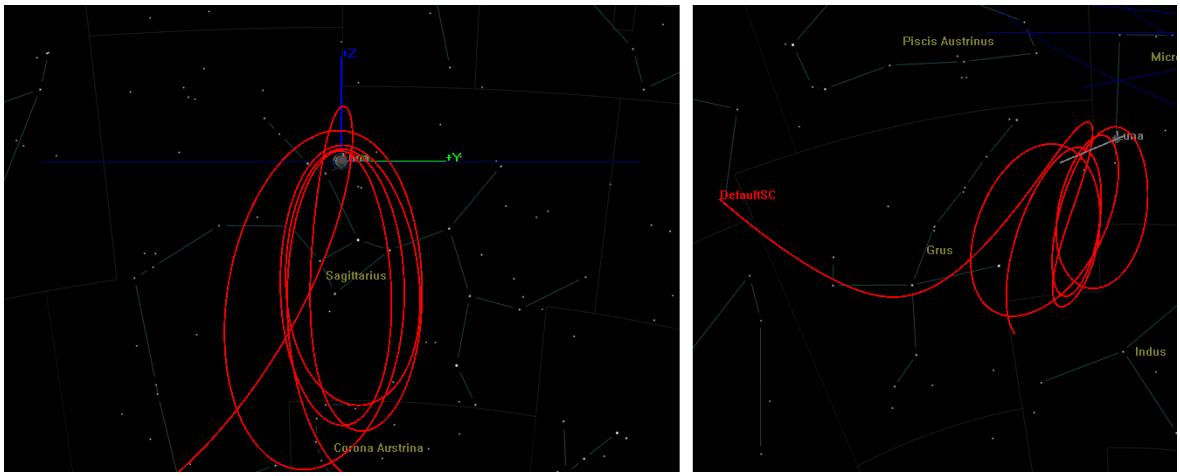

Figure 18 - Stabilized NRHO around the Moon in restricted three-body problem plotted using GMAT

We have deemed this stability satisfactory for transfer maneuvers within the first two orbital periods and we proceeded with attempts to reach DRO. Of note is that the orbit we managed to stabilize is different to the orbit that was used in the transfer network we were using as source for our maneuvers meaning we were already expecting to have to optimize our transfers.

3.4. Leaving NRHO

While our orbit has changed slightly in comparison to the one used in the transfer network and we were certain that effects of the Moon's movement relative to Earth had much larger effect than anticipated, we were still attempting to preserve the initial plan of chaining orbits in NRHO-DRO-L4 SPO chain.

First, we had to determine the optimal location for the impulse burn which we have attempted to position similarly to the transfer network. But we noticed that instead of flying towards a DRO, most of our attempts tended to fly towards the L5 and we decided to study this avenue further. This led to more changes to position of our maneuver and its Δv. We kept decreasing Δv to achieve successful capture into an orbit around L5. This was

best achieved by one impulse burn accelerating the probe by $\Delta v = 150\ \mathrm{m\ s^{-1}}$ as it approaches the midpoint between aposelene and periselene. This allowed the probe to be captured near the L5 into a horseshoe orbit where it remained stable for over half a year. The trajectory of the orbit can be seen in Figure 19

One thing that was detected is that successfully reaching target orbit is heavily dependent on timing of the maneuver. This shows that the trajectory is highly dependent on position of Moon on its trajectory, possibly compounding with its speed relative to Earth.

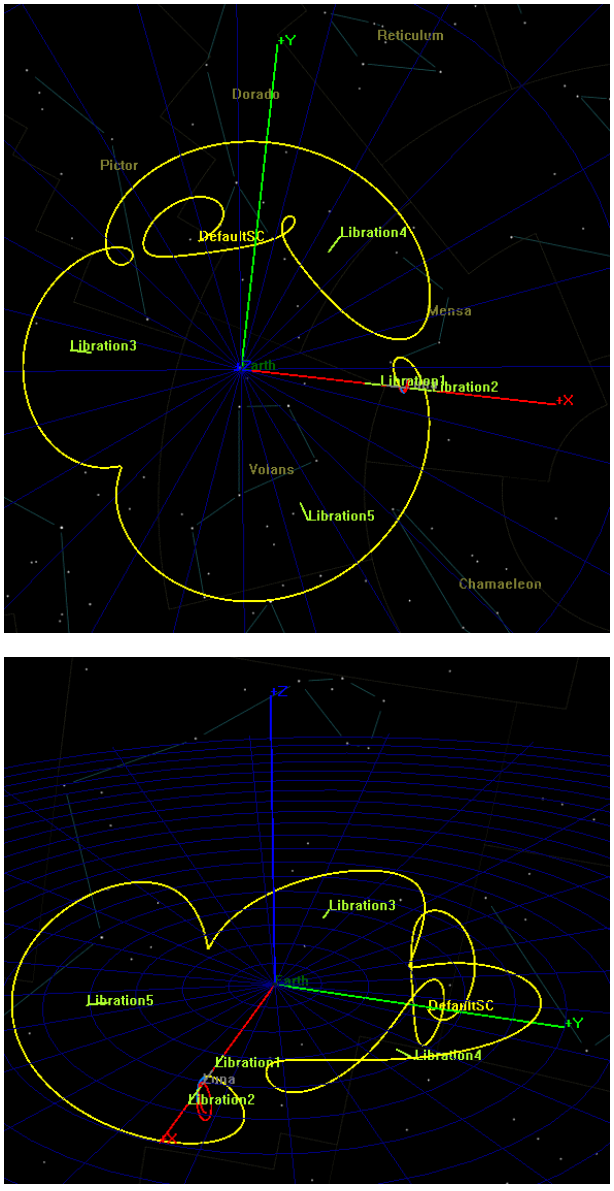

Figure 19 - Direct single-impulse transfer from NRHO to DRO, yellow curve shows trajectory of probe after passing periselene

The yellow curve in Figure 19 is the trajectory of the probe for 160 days after passing periselene and we can clearly see some form of horseshoe orbit which most likely is not very stable. Which is not a problem for us as achieving this orbit only means we can achieve different orbits by adding more impulse maneuvers and altering the current ones.

3.5. Final orbit

As our aim is to spend as much time as possible in the vicinity of L4 or L5 and our current transfer trajectory was taking us into the vicinity of L5, we have decided to aim for an orbit around this point. Our first aim was finding a solution for stable or partially stable orbit around the L5 from which we could attempt to alter the maneuvers in such a way as to obtain a satisfactory orbit. We decided on using intermediate maneuver after passing periselene and optimized position of this maneuver to obtain the closest fly-by of the L5 that we could achieve by varying this factor. We have found during the simulations that we can maintain a considerable level of stability of our solution while moving the maneuver around if we keep the Δv constant.

Our first successful and stable orbit was achieved with two braking burns after leaving the orbit of the Moon. The first braking maneuver happens 10 days after leaving periselene and has $\Delta v = -50\ \mathrm{m\ s^{-1}}$. The second braking maneuver happens when the probe reaches maximum height over the Moon's orbital plane as this point coincides with what could be related to as one of the apsides. When reaching this point the probe performed another braking maneuver with same Δv as the previous one. This appears to land us on very stable orbit around the L5 as shown in Figure 20.

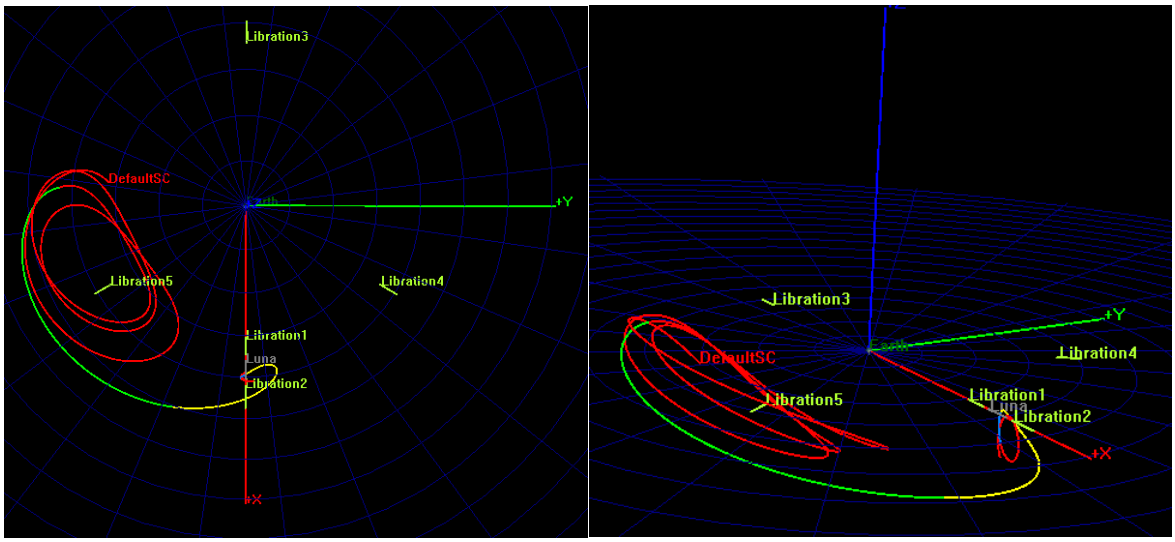

Figure 20 - Our first simulated stable orbit around L5

From this orbit we iterate searching for the optimal time for first braking burn and through several iteration it was brought to 6.5 days after passing the periselene. Further optimization after this required a change in approach. More and more, the movement outside of Moon's orbital plane was affecting the distance to the L5, therefore we had to change the orbital plane at which our probe orbits. While we were attempting to avoid this

maneuver as it is very costly from Δv perspective, it has become necessary to achieve our goals. This also led to lowering Δv of other maneuvers as we need to keep kinetic energy high enough so that curves of zero velocity are close enough to the L5 or non-existent in the vicinity of the L5. We manage to achieve close enough proximity to the L5 at increased Δv cost and loss of stability of our solution, which can be seen in Figure 21.

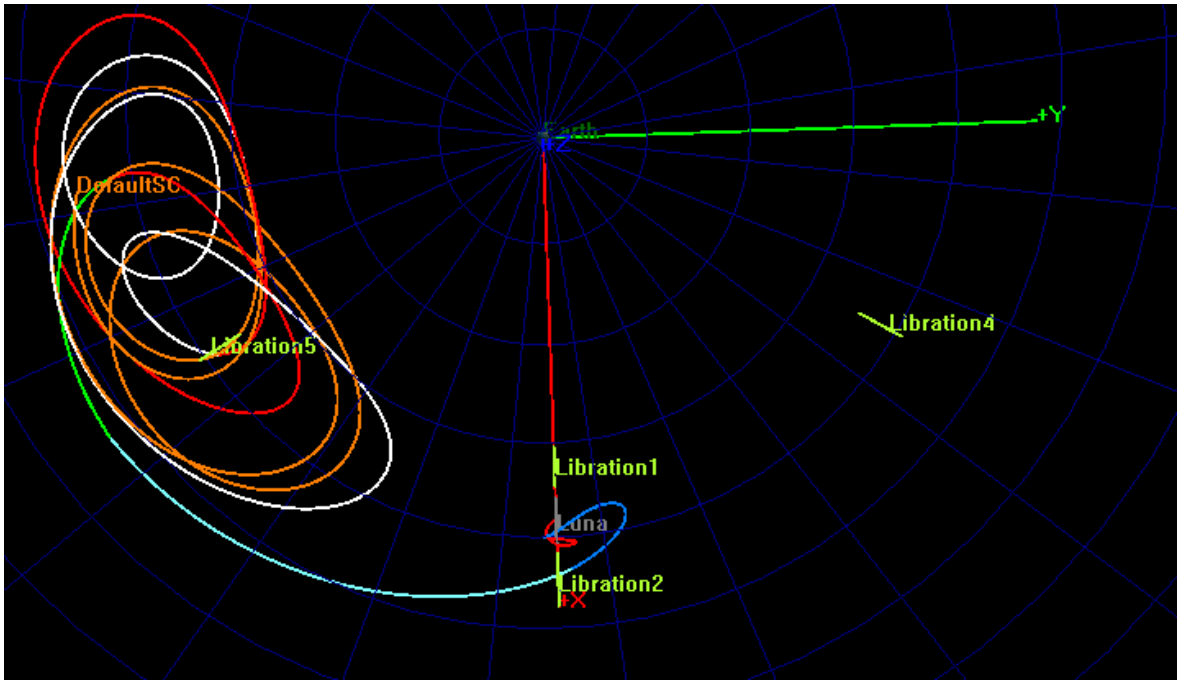

Figure 21 - Unstable orbit around L5 with close fly-bys, change in color of trajectory denotes impulse maneuver, blue between maneuvers 1 and 2, cyan between 2 and 3, green between 3 and 4, red between 4 and 5, white between 5 and 6, and orange after maneuver no. 6

Table 2 - Table of maneuvers used to achieve close fly-bys of L5

No.	Name	Time elapsed	Δv
1	Departure from NRHO	9 days	150 m/s in direction of +Z
2	Circumlunar braking	16.5 days	40 m/s against direction of velocity vector
3	Aligning plane of orbit	26.5 days	150 m/s in direction of -Z
4	Braking for capture near L5	35 days	30 m/s against direction of velocity vector
5	Stabilization burn for close fly-bys	76.75 days	74.15 m/s roughly in direction of +Y
6	First correction burn	157 days	20 m/s in direction of +X
			Total Δv is 464.15 m/s

Probe deorbits after about three months without a correction burn, performing two close fly-bys of L5. These close fly-bys destabilize the orbit and cause the probe to enter a horseshoe orbit with long period. Even on its own this orbit is not ideal as majority of the time is spend far away from the L5 and the correction maneuvers are frequently needed.

3.6. Results

We have created and optimized a transfer trajectory between NRHO and orbit around the L5. There have been several noteworthy results, especially due to their stability with such an inherently unstable system. There was no stable solution found for orbits that venture close enough to the L5 to fulfill mission demands, therefore we had to settle for an unstable solutions with frequent corrections if we are to fulfill the assignment. On the graph we can see distance between probe and L5. Probe first reaches the distance of 20 000 kilometers to the L5 after 66 days in transfer, as shown in Figure 22. The problem with this orbit is that it spends only 3.3% of the time in the vicinity of the L5, but for such close fly-bys no alternative was discovered. As can be seen on the graph, the probe performs several distant orbits before re-entering the neighborhood of the L5. The last third entry just barely misses the needed distance to the L5 meaning that a correction burn will be needed to perform close pass. The relative speed is in low hundreds of meters per second during the fly-bys, as can be seen in Figure 23 and Figure 24. As the specifics of the detection equipment are not available, evaluation of this parameter is not possible. But as far as relative velocities in space go, these are rather low, therefore we can talk about low-speed fly-bys.

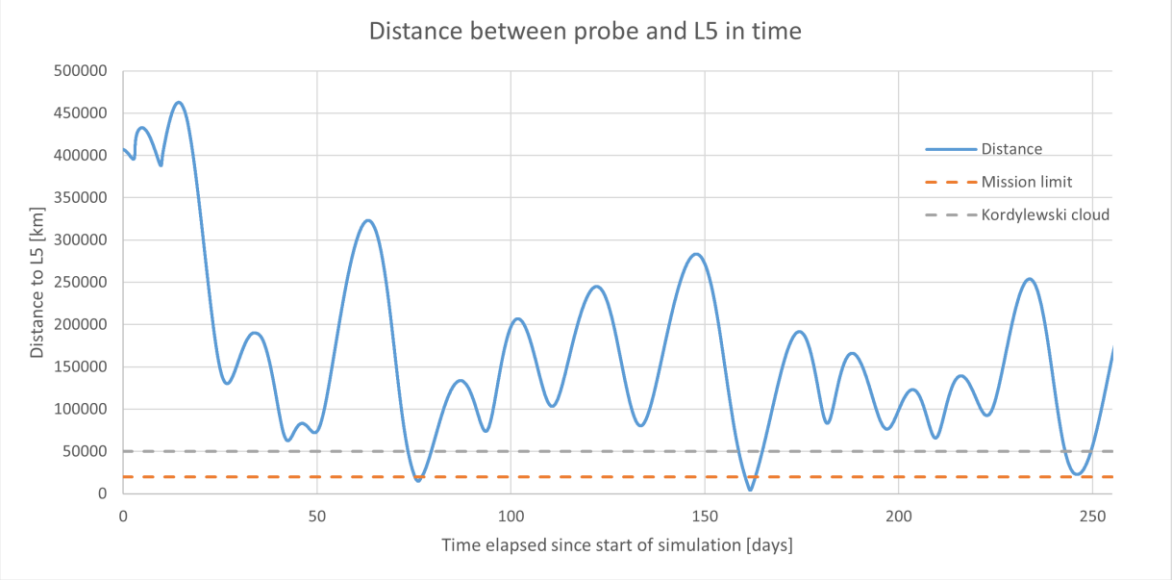

Figure 22 - Graph of distance between probe and L5 on unstable close orbit

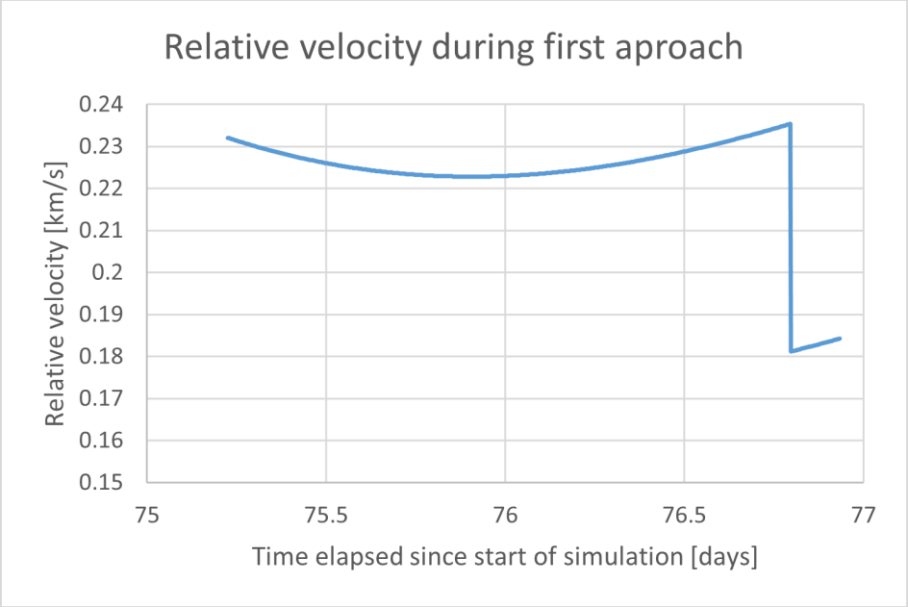

Figure 23 – Graph of relative velocity during first approach of probe to L5

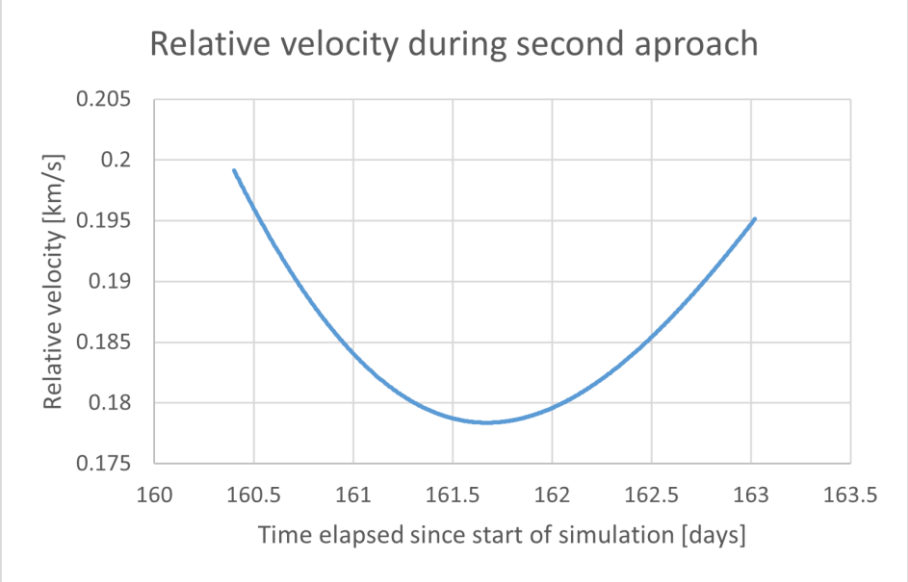

Figure 24 – Graph of relative velocity during second approach of probe to L5

As the mission of the probe is to detect and observe the Kordylewski clouds, we might be interested in other orbits too. From ground-based observations the Kordylewski clouds appear to span area bigger than 100 000 by 70 000 kilometers around the triangular points. [11] Which is a looser limit than 20 000 kilometers specified in this assignment. While some of the more stable orbits come close to those distances none of the orbits discovered in our simulations manages to reach these distances reliably, it might be possible that there could be stable solution for these upper bounds of the Kordylewski clouds theoretically achieving higher percentage of measurement time but none of the solutions we discovered so far achieves that with stable orbits usually normalizing at slightly over 50 000 kilometers in distance from a Lagrange point. But since we didn't explore this option as extensively due to focus on 20 000-kilometer constraint, there might be a yet-undiscovered stable solution that would be viable for the loosened constraints. Our possibly most successful

attempt at such stable orbit can be seen in Figure 25. The distance of the probe to L5 is plotted in Figure 26. The maneuvers used to achieve this orbit can be seen in Table 3. We can also see in Figure 27 that the relative velocity oscillates between 200 m/s and 600 m/s, which is still relatively low velocity.

Table 3 - Table of maneuvers used to achieve a stable orbit of L5

No.	Name	Time elapsed	Δv
1	Departure from NRHO	9 days	150 m/s in direction of +Z
2	Circumlunar braking	16.5 days	40 m/s against direction of velocity vector
3	Aligning plane of orbit	26.5 days	150 m/s in direction of -Z
4	Braking for capture near L5	35 days	40 m/s against direction of velocity vector
			Total Δv is 380 m/s

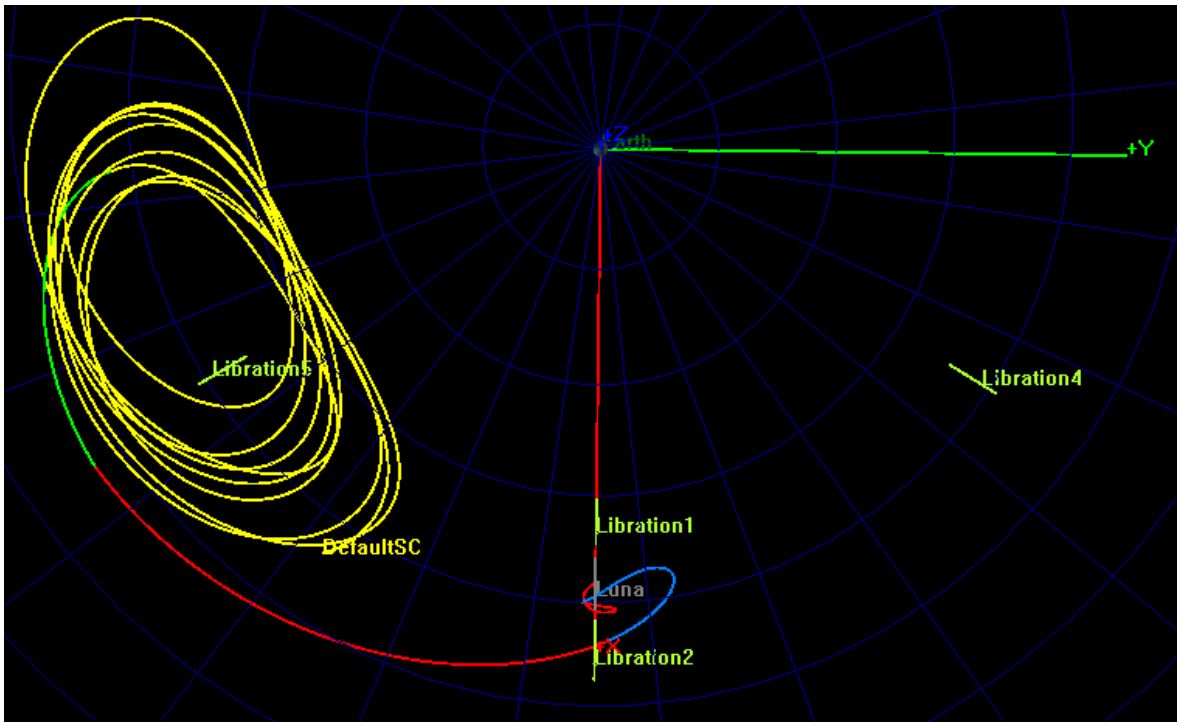

Figure 25 - Stable orbit around L5, the change in color of trajectory denotes impulse maneuver, blue is between maneuvers 1 and 2, red between 2 and 3, green between 3 and 4, and yellow after maneuver 4

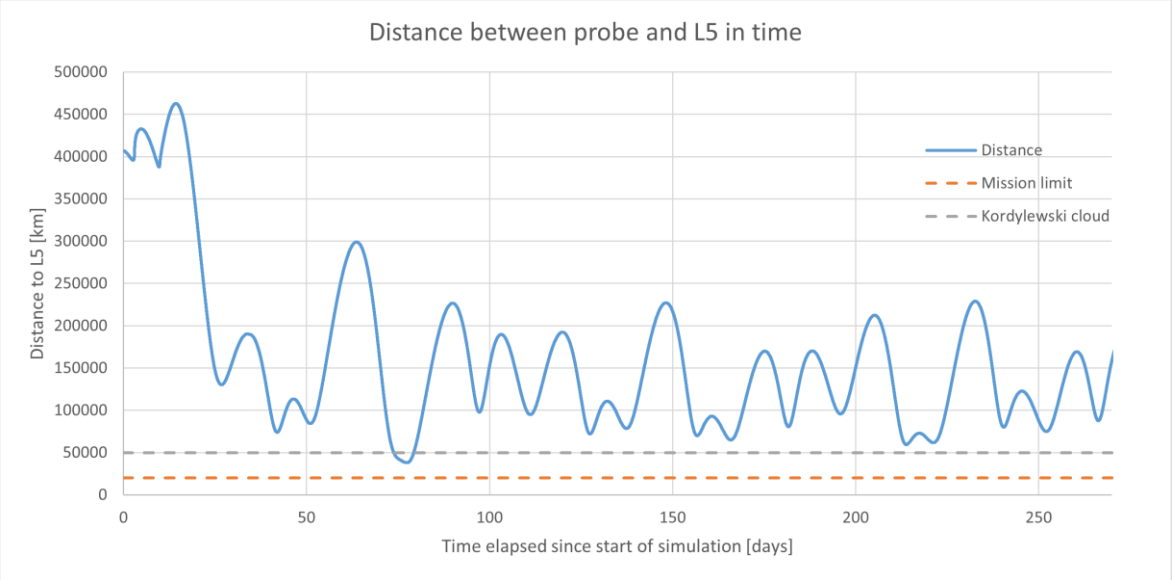

Figure 26 - Graph of distance between probe and L5 on long-term stable orbit

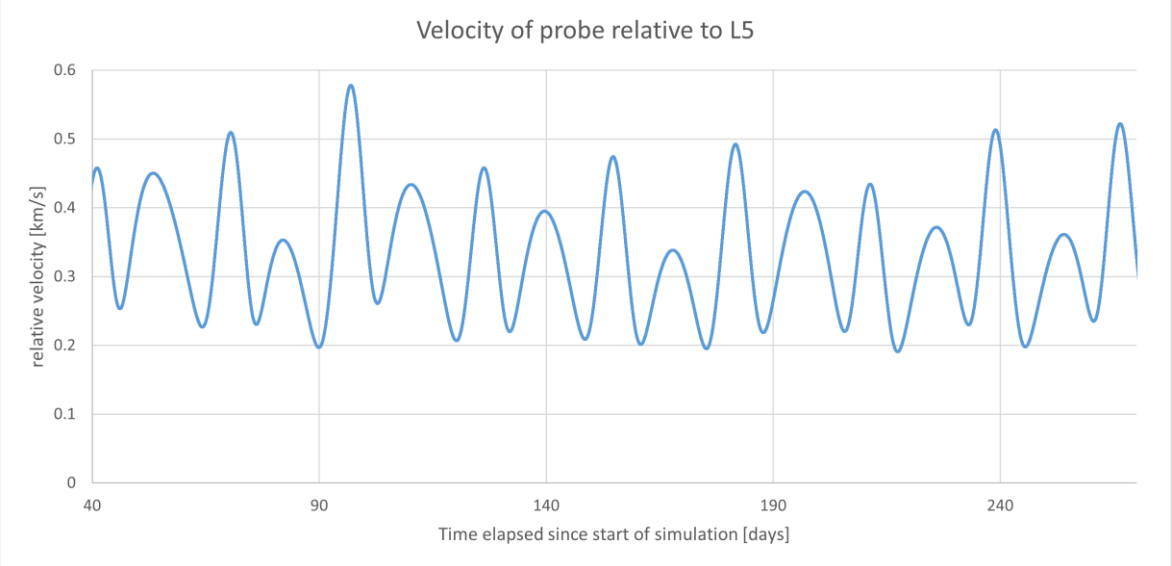

Figure 27 - Relative velocity between L5 and the probe on stable orbit

While outside the scope of original assignment, it is worth noting that all stable orbits found were safely outside of the Kordylewski dust cloud and therefore wouldn't suffer any effects the dust particles could have on them, from loss of kinetic energy due to impacts, to the abrasion of solar panel surfaces. While this observation is detrimental to our mission, it is at the same time dispelling some of the concerns about the dust clouds affecting the viability of the orbits about the triangular points. [4]

4. Discussion

While the accuracy of our simulation is greater than of the predictions made based on circular restricted three-body problem, there can be further disturbances if we look for solution in n-body problem or include solar radiation pressure. While we do not believe the changes will be significant, they might require minor changes to the maneuvers employed.

While there are other options for visiting vicinity of L4 and L5, these options have mostly already been explored in other works. Especially when it comes to transfers from LEO to triangular points, where studies have shown that by traveling close to the Moon such maneuvers can decrease fuel necessary to perform them. As these transfers have already been explored in-depth, we decided to explore other avenues that could lead to new more beneficial flightpaths being found. The same decision was made regarding the orbit used by satellite Hiten. [12]

We have discovered that circular approximation of the three-body problem is not viable for translation into more realistic scenarios using the ephemeris model. This has led to need for correction on NRHO to even achieve temporarily stable orbit and made transfer to DRO or L5 SPO impossible using the maneuvers as outlined in the used transfer network. This meant we had to develop completely new maneuvers that are viable in the ephemeris model used by GMAT. This effectively led to having to rely on the multiple shooting method and slow iterative approach where we manually evaluated every result for its viability. [5]

While in the circular restricted three-body problem there appear to be stable orbits even very close to L4 and L5, we were not able to achieve any such orbit in our simulations. While it is possible that such orbits exist, it appears that the motion of the triangular points introduces disturbances to these orbits. This effect is stronger the closer the probe is to the Lagrange point and as our target distance is 20 000 kilometers, while the linear movement of the Lagrange points is 40 000 kilometers, the effects seem significant. The orbits with better stability managed to only reach a distance of roughly 38 000 km meaning they are not satisfactory for this assignment. Which could still be close enough to detect the Kordylewski dust cloud as those reach over 50 000 kilometers away from the triangular points according to the observations.

The motion also means that epoch of our arrival to the orbit is crucial too, which paired with maneuver to leave NRHO being heavily dependent on epoch too introduces more challenges for the optimization of our transfer.

5. Future plans

While theoretically fulfilling the assignment in its current form, practicality of this solution is dubious at best and therefore more investigation needs to be put into finding viable orbits with high ratio of measurement time. This investigation should consist of creating a script to search for viable orbits around L5 and L4 without regard to their availability from NRHO or LEO. After confirming the existence of stable viable orbits with acceptable measurement time ratio, we will then investigate options of transferring to those specific orbits with respect to launch and arrival epoch.

6. Conclusion

We started with plan on chaining several orbits together using already explored transfer network [5] connecting NRHO to DRO and to L4 SPO. This plan didn't come to fruition as moving from the circular restricted three-body problem into ephemeris model introduced far too many disturbances to achieve the same results as were explored in other papers using circular three-body problem. Therefore, we had to look for our own solutions.

We have discovered and explored transfer possibilities from NRHO to orbits around L5 and found promising transfers and orbits. The total Δv cost of our maneuvers to achieve target orbit is $464.15\ \mathrm{m\ s^{-1}}$, which is lower than the original estimate using transfer network chaining NRHO-DRO-L5 SPO. We have found unstable orbit achieving close fly-bys of the L5 and stable orbits in greater distance. The time from first maneuver to achieving target distance from the L5 is roughly 66 days, which is more than satisfactory, but the Δv cost is rather high, and the orbit has very poor ratio of measurement time to total time of flight, only 3.3% of the time is spent within close enough proximity. This means that while our investigation found promising candidate, we need to investigate its viability and potential improvements over it. We have also found stable orbit on the edge of the Kordylewski dust cloud at the L5 that needs total Δv of only $380\ \mathrm{m\ s^{-1}}$ and is stable for almost a year without any correction burns. Regrettably this orbit only skims over the outer edge of expected span of the Kordylewski dust cloud making this solution less viable.

But the conclusions are not all negative. Some of the positive conclusions are that our simulations confirmed existence of very stable orbits around the L5 within the restricted three-body problem using ephemeris model of Lunar orbit. These orbits remain stable in excess of a year without any need for further correction burns, presenting an interesting parking orbit. Further, these orbits should be safely outside of the Kordylewski dust cloud and therefore safe from any negative effects of the dust particles.

Sources

[1] VALTONEN, Mauri a Hannu KARTTUNEN. *The Three-Body Problem*. Cambridge: Cambridge University Press, 2005. ISBN 978-0-511-13289-6.

[2] KOON, Wang Sang, Martin W. LO, Jerrold E. MARSDEN a Shane D. ROSS. *Dynamical Systems, the Three-Body Problem and Space Mission Design*. 2011. ISBN 978-00-615-24095-4.

[3] DUNBAR, Brian, GARCIA, Mark, ed. International Space Station Facts and Figures. *National Aeronautics and Space Administration* [online]. Nov 4, 2021 [cit. 2022-06-06]. Available at: https://www.nasa.gov/feature/facts-and-figures

[4] SLÍZ-BALOGH, Judit, András BARTA a Gábor HORVÁTH. Celestial mechanics and polarization optics of the Kordylewski dust cloud in the Earth–Moon Lagrange point L5 – Part II. Imaging polarimetric observation: new evidence for the existence of Kordylewski dust cloud. *Monthly Notices of the Royal Astronomical Society*. 2019, 482(1), 762-770. ISSN 0035-8711. doi:10.1093/mnras/sty2630

[5] CAPDEVILA, Lucía R. A *Transfer Network Linking Earth, Moon, and the Triangular Libration Point Regions in the Earth-Moon System*. West Lafayette, 2016. Dissertation. Purdue University.

[6] ZIMOVAN, Emily M., Kathleen C. HOWELL a Diane C. DAVIS. Near Rectilinear Halo Orbits and Their Application in Cis-Lunar Space. In: *3rd IAA Conference on Dynamics and Control of Space Systems*, Vol. 20. Moscow, 2017 [cit. 2022-06-06].

[7] *Solar System Dynamics: Three-Body Periodic Orbits* [online]. NASA [cit. 2022-06-06]. Dostupné z: https://ssd.jpl.nasa.gov/tools/periodic_orbits.html#/periodic

[8] BARRABÉS, E. a S. MIKKOLA. *Families of periodic horseshoe orbits in the restricted three-body problem*. 2005, 432(3), 1115-1129. ISSN 0004-6361. Available at: doi:10.1051/0004-6361:20041483

[9] PRITCHETT, Robert E., Emily ZIMOVAN a Kathleen HOWELL. Impulsive and Low-Thrust Transfer Design Between Stable and Nearly-Stable Periodic Orbits in the Restricted Problem. *2018 Space Flight Mechanics Meeting*. Reston, Virginia: American Institute of Aeronautics and Astronautics, 2018, 2018-01-08, -. ISBN 978-1-62410-533-3. doi:10.2514/6.2018-1690

[10] HUGHES, Steven P. a Darrel J. CONWAY. *Using the General Mission Analysis Tool (GMAT)* [online]. [cit. 2022-06-06]. Available at: https://ntrs.nasa.gov/citations/20170001580

[11] FAZEKAS, Andrew. *National Geographic: Earth has two extra, hidden 'moons'* [online]. 2018 [cit. 2022-06-06]. Available at: https://www.nationalgeographic.com/science/article/news-earth-moon-dust-clouds-satellites-planets-space

[12] *NASA Space Science Data Coordinated Archive: Hiten* [online]. [cit. 2022-06-06]. Available at: https://nssdc.gsfc.nasa.gov/nmc/spacecraft/display.action?id=1990-007A

List of figures

List of tables

List of appendixes

Appendix 1 - GMAT script for simulation of unstable orbit with close fly-bys of L5 named "Appendix1_NRHO-L5_unstable.script"
Appendix 2 - Data output of GMAT simulation containing location, velocity, and acceleration of probe, location, and velocity of L5, and position of Moon in file named "Appendix2_Unstable_L5_orbit.txt"
Appendix 3 - GMAT script for simulation of stable orbit around L5 named "Appendix3_NRHO-L5_stable.script"
Appendix 4 - Data output of GMAT simulation containing location, velocity, and acceleration of probe, location, and velocity of L5, and position of Moon in file named "Appendix4_Stable_L5_orbitfigure 4"